Van Zonneveld, A. J., Veerman, H., & Pannekoek, H. (1986b) *Proc. Natl. Acad. Sci. U.S.A. 83*, 4670–4674.
Verheijen, J. H., Caspers, M. P. M., Chang, G. T. G., de Munk, G. A. W., Pouwels, P. W., & Enger-Valk, B. E. (1986) *EMBO J. 5*, 3525–3530.
Wang, B.-C. (1985) in *Methods in Enzymology* (Wyckoff, H. W., Hirs, C. H. W., & Timasheff, S. N., Eds.) Vol. 115, Part B, pp 90–112, Academic Press, Orlando, FL.
Weening-Verhoeff, E. J. D., Quax, P. H. A, Van Leeuwen, R. T. J., Rehberg, E. F., Marotti, K. R., & Verheijen, J. H. (1990) *Protein Eng. 4*, 191–198.
Wilmot, C. M., & Thornton J. M. (1988) *J. Mol. Biol. 203*, 221–232.
Winn, E. S., Hu, S.-P., Hochschwender, S. M., & Laursen, R. A. (1980) *Eur. J. Biochem. 104*, 579–586.
Wu, T.-P., Padmanabhan, K., Tulinsky, A., & Mulichak, A. M. (1991) *Biochemistry 30*, 10589–10594.
Wyckoff, H. W., Doscher, M., Tsernoglou, D., Inagami, T., Johnson, L. N., Hardman, K. D., Allewell, N. M., Kelly, D. M., & Richards, F. M. (1967) *J. Mol. Biol. 27*, 563–578.

Lipid Polymorphism: A Correction. The Structure of the Cubic Phase of Extinction Symbol *Fd--* Consists of Two Types of Disjointed Reverse Micelles Embedded in a Three-Dimensional Hydrocarbon Matrix†

Vittorio Luzzati,*,‡ Rodolfo Vargas,‡ Annette Gulik,‡ Paolo Mariani,§ John M. Seddon,∥ and Emilio Rivas⊥

Centre de Génétique Moléculaire, Laboratoire Propre du CNRS Associé à l'Université Pierre et Marie Curie, 91198 Gif-sur-Yvette, France, Istituto di Fisica Medica, Università di Ancona, Via Monte d'Ago, 60100 Ancona, Italy, Department of Chemistry, Imperial College, London SW7 2AY, U.K., and Instituto de Biología Celular, CONICET, Buenos Aires, Argentina

Received April 17, 1991; Revised Manuscript Received September 17, 1991

ABSTRACT: The X-ray scattering study of a cubic phase of extinction symbol *Fd--*, recently performed on a lipid extract (PFL) from *Pseudomonas fluorescens* [Mariani et al. (1990) *Biochemistry 29*, 6799–6810] has been extended to several other systems, all consisting of mixtures of water-miscible (MO, PC, PE, oleate) and of water-immiscible (FA, DG) lipids, plus water. In all of these systems the cubic phase was observed in the presence of excess water. Some inconsistencies observed between PFL and the other systems, the fact that in PFL one of the reflections of the cubic phase happened to coincide with the strongest reflection of the hexagonal phase, and the finding, in one of the original cubic samples of PFL kept in the cold for more than 3 years, that the intensity of one of the reflections had decreased dramatically all indicated that a nonnegligible amount of a hexagonal impurity was in fact present in the samples of PFL originally thought to contain a pure cubic phase. The intensities were corrected for that impurity and analyzed again using a pattern recognition approach based upon the axiom that the histogram of the electron density maps is invariant with respect to physical structure, when different phases are compared whose chemical composition is the same. The hexagonal phase provided the reference phase for the comparison. The moments $\langle(\Delta\rho)^n\rangle$ were used to compare the histograms. All the phase combinations (the φ-sets) compatible with the data were generated and were screened using the distance between the points of the cubic and the hexagonal phases in the 6D space of the moments ($[\langle(\Delta\rho)^n\rangle]^{1/n}$), with $n = 3$–8. The result of the analysis is a structure formed by two types of disjointed micelles of type II (water-in-oil), quasi-spherical in shape: eight (per F-centered cubic cell), of symmetry $\bar{4}3m$, are centered at positions a, and 16, of symmetry $\bar{3}m$, are centered at positions d [according to the *International Tables* (1952)]. This structure has previously been proposed by Charvolin and Sadoc (1988) on the basis of formal geometric arguments. The study of the cubic phase of the other lipid systems is hindered by the lack of a reference phase; the structure was analyzed by reference to the cubic phase of PFL and found to be the same in all the systems. This cubic phase is the first example, among lipid-containing phases, of a 3D periodically ordered micellar organization of type II.

A face-centered cubic phase of extinction symbol *Fd--* (cubic aspect 15; phase Q_{15}, according to our notation) was discovered by Tardieu (1972) in a lipid extract from *Pseudomonas fluorescens*, provided by E. Rivas. For a long time no other example of that phase was reported in any lipid-containing system. Quite recently, a renewed interest in cubic phases has stimulated a more systematic search that has uncovered several additional examples of that phase: MO–OA–water[1] (Mariani et al., 1988, 1990), DOPC–DOG–water (Seddon, 1990), NaO–OA–water (Seddon et al., 1990a), PE–DOG (Gulik and Vargas, unpublished work), some ill-

† This work was supported in part by grants from the Association Française pour la Recherche Médicale, the Ligue Nationale Française contre le Cancer, and the Science and Engineering Research Council (U.K.) (Research Grant GR/C/95428). One of us (R.V.) was supported by a postdoctoral grant from the Association Française pour la Recherche Médicale.

‡ Laboratoire Propre du CNRS Associé à l'Université Pierre et Marie Curie.
§ Università di Ancona.
∥ Imperial College.
⊥ CONICET.

[1] Abbreviations: PFL, lipid extract from *Pseudomonas fluorescens* (Mariani et al., 1990); MO, monoolein; FA, fatty acid; OA, oleic acid; MA, myristic acid; NaO, sodium oleate; PC, phosphatidylcholine (lecithin); PE, phosphatidylethanolamine; DOPC, dioleoylphosphatidylcholine; DMPC, dimyristoylphosphatidylcholine; DG, diacylglycerol; DOG, dioleoylglycerol. The lipids are arranged in two classes: water-miscible are those (PFL, MO, NaO, PC, PE, DOPC, DMPC) that display water-containing phases, and water-immiscible are the others (FA, OA, MA, DG, DOG).

0006-2960/92/0431-279$03.00/0

Table I: Experimental Data Relevant to Phase Q^{227} [a]

lipid:	PFL	PFL		PFL		MO–OA	MO–OA	MO–OA	DOPC–DOG	NaO–OA	DMPC–MA	PE–DOG
expt no.:	1	2		3		4	5	6	7	8	9	10
c		0.91		0.86			*0.71*	*0.60*	*0.85*			
$c_{v,pol}$		0.25		0.29			*0.36*	*0.47*				
T (°C)	60	60		60		25	20	40	33	30	54	42
a (Å)	125.8	129.6		146.2		134.0	139.8	166.9	156.4	155.0	170.1	134.3
$h^2 + k^2 + l^2$							normalized intensity values (I_{obs})					
3	20	*3*	8	*3*	7	13	5	*9*	5	17	20	10
8	215	*77*	194	*75*	178	150	209	*63*	133	162	144	149
11	561	*285*	539	*275*	512	490	362	*248*	419	457	499	406
12	162	(*586*)	157	(*583*)	148	146	188	(*255*)	77	102	203	180
16	23	*15*	38	*18*	43	42	58	*36*	50	45	60	47
19	18	*10*	24	*11*	24	29	44	*49*	54	54	73	53
24		*3*	7	*3*	7	24	29	*40*	65	35		26
27		*6*	16	*9*	21	40	35	*59*	82	50		41
32		*4*	11	*7*	17	32	29	*71*	66	38		45
35		*0*	0	*4*	9	0	0	*0*	0	0		0
36		*0*	0	*2*	5	0	4	(*59*)	0	0		0
40		*2*	6	*5*	12	11	1	*0*	0	0		13
43				*3*	7	0	4	*0*	} 48	} 30		0
44				*3*	9	24	17	*43*				28
48								(*74*)				

[a] c, weight concentration (lipid/sample); $c_{v,pol}$, volume concentration of the polar moiety; T, temperature; a, lattice parameter of the cubic cell; I_{obs} normalized intensity ($\sum_h I_{obs}$ (**h**) = 1000) of the Debye–Scherrer ring of spacing $(h^2 + k^2 + l^2)^{1/2}/a$. PFL: experiment 1, this work (see text); experiments 2 and 3, Mariani et al. (1990) (note that the exposure time of experiment 2 happened to be much shorter than that of experiment 3 and that, as a consequence, the weakest reflections were not observed). MO–OA: experiment 4, this work; experiments 5 and 6, experiments 9 and 10 of Mariani et al. (1988). DOPC–DOG: experiment 7, Seddon (1990). NaO–OA: experiment 8, Seddon et al. (1990a). DMPC–MA and PE-DOG: experiments 9 and 10, this work. Empty cases and figures in italics correspond respectively to missing and to inaccurate (or obsolete) data. In parentheses are intensities originally ascribed to the cubic phase which contain, in fact, a substantial contribution from a hexagonal phase (see text).

defined cosmetic preparations (Gulik-Krzywicki, unpublished work), a mixture of phosphatidylcholine, phosphatidylethanolamine, diacylglycerol, cholesterol, and water (Nieva, unpublished work). At present Q_{15} appears to be a most common phase in systems containing FA or DG, in addition to water-miscible lipids (PC, PE, MO, oleate). In all the examples known so far, the water content of the phase is small (Table I); as a rule, moreover, and with the conspicuous exception of PFL, the cubic phase is observed in equilibrium with excess water. We have tackled recently (Mariani et al., 1990) the structure analysis of that phase.

The fact must be stressed that the structure analysis of lipid phases is a peculiar game whose rules are not quite the same as those that prevail in ordinary crystallographic analyses (Mariani et al., 1988). The data are the space group (or a small number of possible space groups), the dimensions of the unit cell, the chemical composition of the phase, its position in the phase diagram, and the intensity of the reflections. The number of observed reflections is intrinsically small (usually less than 20) because of the presence of short-range disorder. Standard crystallographic techniques are of little help to determine the structure of these phases: heavy-atom derivatives are rarely available, and the possibility of calculating the structure factors is severely restricted by the complex shapes of the structure elements. More useful criteria are the analogies with other phases of the same (or of a similar) system: the electron density maps must make good chemical sense, the dimensions of the structure elements must be compatible with the chemical nature of the system, etc. In some cases, moreover, additional information is provided by electron microscopy and spectroscopic experiments. In order to circumvent some of the problems, we have resorted to a pattern recognition technique based upon the axiom that the histogram of the electron density map is far more sensitive to the chemical composition of the phase (namely, the nature of the lipid and the amount of water) than to its physical structure (Luzzati et al., 1988; Mariani et al., 1988). More precisely, we have assumed that in phases of different structure and equal chemical composition the parameter $\langle(\Delta\rho)^4\rangle$ (see eq 1), which is a function of the histogram of the map, is invariant.

From the practical viewpoint, we operate on the moduli of the structure factors $|F(\mathbf{h})|$. After scale and shape normalizations and after setting $F(0) = 0$, we generate all the phase combinations—the φ-sets—compatible with the data and compute the corresponding values of $\langle(\Delta\rho)^4\rangle$. If another lipid phase of known structure is available whose chemical composition is the same as that of the unknown phase, then we seek the φ-set (or sets) whose parameter $\langle(\Delta\rho)^4\rangle$ is close to that of the reference phase.

The technique has been used successfully in the study of a variety of lipid systems (Mariani et al., 1988). PFL–water seemed to be a highly favorable case since the phase Q_{15} is observed over a narrow concentration range, straddled by a hexagonal phase (Mariani et al., 1990). An obvious pitfall, intrinsic to chemical complexity, is that more than one phase may be present in any one sample. We tried to evade the danger by carefully exploring the regions of the phase diagram ascribed to each of the phases [see Figure 1 in Mariani et al. (1990)]. A better alternative would be to concentrate one's effort on systems of simpler chemical composition (see Table I); yet the absence of other phase(s) of known structure and of composition close to that of Q_{15}, and thus the lack of a reference value of $\langle(\Delta\rho)^4\rangle$, have so far precluded that approach.

The result of the analysis was a structure of space group $Fd3m$ (Q^{227} in our notation), formed by a 3D network of rods, tetrahedrally joined 4 by 4 according to a diamond lattice, and of a family of quasi-spherical disjointed micelles centered at positions d (*International Tables*, 1952). Rods and micelles were supposed to be filled by the polar medium (structure of type II). That structure, which was in excellent agreement with the crystallographic data available at that time, was also found to fulfill several chemical criteria that are not involved in the crystallographic analysis: the volume of the structure

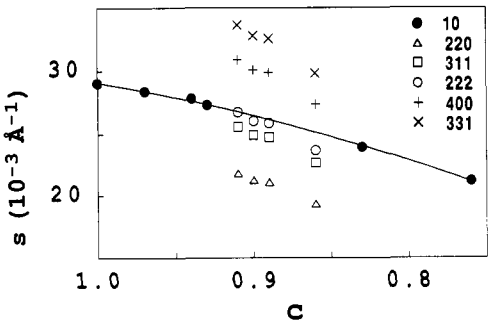

FIGURE 1: Hexagonal (H) and cubic (Q^{227}) phases of PFL: spacings of the observed reflections as a function of concentration. Note that the observed spacing of the reflection (222) of phase Q^{227} is very near to the interpolated spacings of the reflection (10) of phase H (full line). Note also [see Table III in Mariani et al. (1990)] that over the concentration range of phase Q^{227} the reflection (10) is much stronger than all the other reflections of phase H.

elements is consistent with the volume occupied by the polar moiety, the area per chain at the polar–apolar interface agrees with other systems, and the dimensions of the apolar regions are compatible with the length of the hydrocarbon chains.

All of the evidence regarding phase Q_{15} of PFL thus seemed to agree with the rod-and-micelle model. On the other hand, nevertheless, the crystallographic data relevant to the phase Q_{15} of other systems were difficult to fit to that model (Mariani et al., 1988). One of us (Seddon, 1990) discussed the problem in the case of PC–DG and suggested that the structure might, in that case, agree with a proposal put forward by Charvolin and Sadoc (1988) (see below). Since the relative intensity of the reflections is quite similar in the different systems (with the exception of PFL; see Table I), we decided to undertake in the case of experiment 7 the tedious task of generating all the φ-sets and of screening the electron density maps, in a search for a structure similar to that adopted for PFL. Much to our surprise, none of the φ-sets within the half with the smallest values of $\langle(\Delta\rho)^4\rangle$ was found to yield a map consistent with the rod-and-micelle model. There were two possible explanations: either cubic phases with the same extinction symbol can have different structures in different systems, or the structure originally proposed for PFL is incorrect.

Apparently (see Table I), the discrepancy is focused on the reflection (222), which is much stronger in PFL than in all the other systems. Besides, the position of the first reflection of the hexagonal phase of PFL, extrapolated to the concentration of the cubic phase, happens to fall almost exactly on top of the reflection (222) of the phase Q_{15} (Figure 1). The suspicion thus arose that the samples of PFL originally diagnosed as "cubic" might in fact contain a nonnegligible amount of hexagonal phase (the fact that the hexagonal phase had escaped the polarizing microscope inspection could be explained by the deep color and the turbidity of PFL preparations). By a fortunate accident, a few sample holders containing the original cubic phase samples of PLF had been preserved in the cold (at approximately −15 °C) for more than 3 years.[2] We tested those samples by X-ray scattering techniques; in one we observed, at 60 °C, the spectrum of phase Q_{15}, with a = 125.8 Å. Besides, *the relative intensity of the reflection (222) had become much weaker than in the original experiments*. An inspection of the data of Table I also shows that in one of the samples of the system MO–OA–water (no. 6), originally ascribed to phase Q_{15} [experiment 10 in Mariani et al. (1988)], the intensity of the reflections (222), (442), and (444) is abnormally high with respect to the same reflections of other systems. Since the spacing ratios of those reflections are $1/\sqrt{3}/2$, that observation corroborated the suspicion that a hexagonal phase, epitaxially related to the cubic phase, might also be present in that sample.

The conclusion could not be escaped that something was wrong with the original data of PFL and MO–OA [experiment 10 in Mariani et al. (1988)] that we had ascribed to phase Q_{15}. More precisely, a nonnegligible amount of hexagonal phase seemed to be present in the samples. Fortunately, it was possible in PFL to eliminate the contribution of that spurious phase from the data and to undertake anew the structure analysis. We used for that purpose an improved version of the previous approach. Moreover, we thought it advisable to carry out in parallel the analysis of all the examples of phase Q_{15} whose crystallographic data were available to us (Table I).

Methods

The chemical procedures, the X-ray scattering techniques, the crystallographic methods, and the notation are those described by Mariani et al. (1990). A few improvements have been introduced in the mathematical analysis.

(*a*) *Analysis of the Histograms*. The procedure is based upon the comparison of the histograms of the maps $\Delta\rho(\mathbf{r})$ relevant respectively to the phase X under investigation and to a reference phase A whose structure is known; the two phases, moreover, have the same chemical composition. The comparison involves the moments of the histogram:

$$\int_{-\infty}^{\infty}(\Delta\rho)^n\mathrm{H}(\Delta\rho)\,\mathrm{d}(\Delta\rho) = (1/V)\int_v[\Delta\rho(\mathbf{r})]^n\,\mathrm{d}v_\mathbf{r} = \langle(\Delta\rho)^n\rangle \quad (1)$$

Since the moments of order 1 and 2 are fixed beforehand ($\langle(\Delta\rho)\rangle = F(0) = 0$; $\langle(\Delta\rho)^2\rangle = 1$), only the moments of order $n \geq 3$ are involved in the analysis. The previous applications (Luzzati et al., 1988; Mariani et al., 1988, 1990) were restricted to the moment of order 4 (which is also related to the "entropy" of the map). We use here a more sensitive test, namely, the distance $\mathrm{R}_{\mathrm{H},n}$ between the points X and A in the $(n-3)$D space $\{\langle(\Delta\rho)^3\rangle^{1/3}, \langle(\Delta\rho)^4\rangle^{1/4}, \ldots, \langle(\Delta\rho)^n\rangle^{1/n}\}$:

$$\mathrm{R}_{\mathrm{H},n} = \{\textstyle\sum_{m=3}^{n}[\langle(\Delta\rho_\mathrm{A})^m\rangle^{1/m} - \langle(\Delta\rho_\mathrm{X})^m\rangle^{1/m}]^2\}^{1/2} \quad (2)$$

with $n = 8$. This choice and other technical aspects of the computation of $\langle(\Delta\rho)^n\rangle$ will be discussed elsewhere.

(*b*) *An Index of Local Sphericity*. Given a 3D electron density map $\rho(\mathbf{r})$, we wish to estimate how close to spherical symmetry is the portion of the map contained inside a sphere of radius R_j, centered at the point $\mathbf{r}_j$. We introduce the following "index of local sphericity":

$$\Phi(\mathbf{r}_j,R_j) = 1 - \int_0^{R_j}R^2\langle\langle\rho(\mathbf{r}-\mathbf{r}_j)\rangle\rangle^2\,\mathrm{d}R \Big/ \int_0^{R_j}R^2\langle\langle\rho^2(\mathbf{r}-\mathbf{r}_j)\rangle\rangle\,\mathrm{d}R \quad (3)$$

where $\langle\langle f(\mathbf{r}-\mathbf{r}_j)\rangle\rangle$ is the average of the function $f(\mathbf{r})$ over the surface of a sphere of radius $\mathbf{R} = \mathbf{r} - \mathbf{r}_j$, centered at the point $\mathbf{r}_j$:

$$\langle\langle\rho(\mathbf{r}-\mathbf{r}_j)\rangle\rangle = (1/V)\textstyle\sum_\mathbf{h}\mathbf{F}(\mathbf{h})\exp(-2\pi i\mathbf{r}_j\mathbf{s}_\mathbf{h})\,\langle\langle\exp(-2\pi i\mathbf{R}\mathbf{s}_\mathbf{h})\rangle\rangle =$$
$$(1/V)\textstyle\sum_\mathbf{h}\mathbf{F}(\mathbf{h})\cos(2\pi\mathbf{r}_j\mathbf{s}_\mathbf{h})\sin(2\pi Rs_\mathbf{h})/(2\pi Rs_\mathbf{h}) \quad (4)$$

$$\langle\langle\rho^2(\mathbf{r}-\mathbf{r}_j)\rangle\rangle =$$
$$(1/V)^2\textstyle\sum_\mathbf{h}\mathbf{F}_2(\mathbf{h})\cos(2\pi\mathbf{r}_j\mathbf{s}_\mathbf{h})\sin(2\pi Rs_\mathbf{h})/(2\pi Rs_\mathbf{h}) \quad (5)$$

[2] Although the state of water in the sample under the conditions of storage was not tested experimentally, the fact that, upon raising of the temperature to 60 °C, the system quickly reached equilibrium suggests that the water did not freeze out.

The determination of $\Phi(\mathbf{r}_j,R_j)$ is straightforward when the amplitudes and phases of $\mathbf{F}(\mathbf{h})$ are known. The limiting values of $\Phi(\mathbf{r}_j)$ are 0 for perfect symmetry ($\langle\langle\rho(\mathbf{r}-\mathbf{r}_j)\rangle\rangle^2 = \langle\langle\rho^2(\mathbf{r}-\mathbf{r}_j)\rangle\rangle$) and 1 for total lack of symmetry ($\langle\langle\rho(\mathbf{r}-\mathbf{r}_j)\rangle\rangle = \langle\rho(\mathbf{r})\rangle = 0$).

Equations 3–5 will be applied to the points a and d of coordinates $\{^1/_8,^1/_8,^1/_8\}$ and $\{^1/_2,0,0\}$ [*International Tables* (1952) with origin at point $\bar{3}$m], which, as discussed below, coincide with the centers of the globular micelles. The limits of integration in eq 3 correspond to the radii of the spheres centered at the points a and d which are in contact with each other, namely, $R_a = 0.2165a$, and $R_d = 0.1767a$.

Results

Lipid Samples and Data Collection

Q_{15} seems to be one of the most common phases in hydrated systems containing FA or DG, in addition to water-miscible lipids (PC, PE, MO, oleate). As a rule, this cubic phase is observed in the presence of excess water; however, the amount of water within the phase is generally small (Table I). Reproducing the experimental conditions is not as easy with this phase as with other lipid phases: the phase diagrams sometimes behave in an erratic way, the approach to equilibrium is abnormally slow, and strong diffuse scattering is sometimes observed in the X-ray spectra. These phenomena may well be due to the narrow range of chemical composition required for the stability of the phase. Metastability could also be invoked, a phenomenon not unusual in lipid systems when cubic phases are involved (Gulik et al., 1985; Shyamsunder et al., 1988; Caffrey, 1989).

The crystallographic analysis was carried out on a variety of lipid systems.

PFL. We were reluctant to undertake a new extraction since we knew from previous experience that the chemical composition, and thus the phase properties of the lipid extract, are not always reproducible. Besides, we were hesitant to rely upon the concentration determined on the unique sample recovered after 3 years in a refrigerator (experiment 1). Therefore, we decided to use the new experiment (no. 1) to correct the intensity of the reflection (222) of the old data (experiments 2 and 3). We assumed, for that purpose, that in experiments 2 and 3 no other reflection, besides (222), is affected by the hexagonal impurity and that the ratio $I_{222}/(I_{220} + I_{311} + I_{400} + I_{331})$ takes the same value in experiments 1, 2, and 3. These assumptions are justified by the observations that in experiments 1, 2, and 3, and more generally in all the experiments of Table I, the intensity ratios of the first (and strongest) reflections (220), (311), (400), and (331) are very close to each other and that over the concentration range of the cubic phase the reflections of the hexagonal phase, except (10), are all very weak [Table III of Mariani et al. (1990)]. The sets of corrected intensities are reported in Table I. We also assumed that the water content of the cubic phase is not significantly different from that of the whole sample (see Figure 1).

MO–OA. A careful study of MO–OA mixtures in various proportions and at different pH values led us to confirm experiment 9 of Mariani et al. (1990) (labeled no. 5 here) and to question experiment 10 of the former work (see above). A new sample of phase Q_{15} is labeled no. 4 in this work.

DOPC–DOG. The phase Q_{15} of this system in excess water has been studied by Seddon (1990). The intensities used in this work (experiment 7) were measured from his data.

DMPC–MA. This system has been studied by Heimburg et al. (1990), although the phase Q_{15} was not identified by those authors nor by a neutron scattering study (Seddon et al., 1990b). We obtained this phase (experiment 9) at fixed temperature within a very narrow temperature range (around 54 °C), using the same lipid mixture as reported by those authors. This system clearly requires further characterization as a function of fatty acid mole fraction and of hydration to resolve these discrepancies.

PE–DOG. In this system the phase Q_{15} was observed in excess water and with a variable proportion of DOG, over a temperature range dependent upon the DOG content (Gulik and Vargas, unpublished work) (experiment 10).

Miscellanea. Phase Q_{15} was observed by Seddon (Seddon et al., 1990a) in a fully hydrated NaO–OA mixture (experiment 8), by T. Gulik-Krzywicki in an ill-defined cosmetic preparation (private communication) and by J. L. Nieva in a PC–PE–DOG–cholesterol mixture (unpublished observation).

Structure Analysis

Two space groups, *Fd*3 and *Fd*3*m*, are compatible with extinction symbol *Fd*- - (*International Tables*, 1952). For reasons discussed elsewhere (Mariani et al., 1988) we adopt the space group of highest symmetry (Q^{227} in our notation).

The procedure used to screen the φ-sets of each of the cubic samples is based upon a comparison with the virtual hexagonal phase (namely, the phase H extrapolated to the concentration of the cubic phase; Mariani et al., 1990). The comparison was carried out on the most accurate of the two experiments, at $c = 0.86$ (no. 3). The intensities of phase H were apodized as described in Table II of Mariani et al. (1990); for phase Q^{227} the values of the parameter $2\beta^2$ is given in Table II. Moreover, the intensity ratio of the pair of reflections (511) and (333)—which merge in the Debye–Scherrer ring ($h^2 + k^2 + l^2 = 27$)—was chosen as discussed by Mariani et al. (1990).

As for the cubic phase, once the (apodized) moduli of the structure factors are known the φ-sets can be generated and the corresponding values of the $\langle(\Delta\rho)^n\rangle_Q$ determined, for $3 \geq n \geq 8$. Since the signs of the reflections of phase H are known (Mariani et al., 1990), the values of the $\langle(\Delta\rho)^n\rangle_H$ can also be determined. Therefore, the "distance" $R_{H,8}$ (eq 2) of the points corresponding to each of the φ-sets of the cubic phase to the unique point of the hexagonal phase can be computed. The results are presented in Figure 2. Clearly, the parameter $R_{H,8}$ is far more sensitive than $\langle(\Delta\rho)^4\rangle$ to select the φ-set of the cubic phase; indeed, although the minimum of $R_{H,8}$ falls in the region where the values of $\langle(\Delta\rho)^4\rangle$ are the closest, the values of $R_{H,8}$ are widely scattered within a narrow range of $\langle(\Delta\rho)^4\rangle$. *We thus decided to adopt as "best" the φ-set whose $R_{H,8}$ is minimum.* Also reported in the figure are the values of the indices of local sphericity Φ_d and Φ_a (eq 3) as a function of $R_{H,8}$, showing that all, or most of, the maps corresponding to a small value of $R_{H,8}$ display a high degree of local sphericity around the points a and d. Similar results were obtained with experiment 2 of PFL (results not shown).

The crystallographic data relevant to the phase Q^{227} of other systems are reported in Tables I and II. Those data were analyzed adopting the same ratio $I(333)/I(511)$ as for PFL, without apodization. The fact that the reflections (220), (311), (222), (400), and (331) are all fairly strong and that their intensity ratios are almost the same in all the systems (Table I) led us to assume that their signs are the same as for experiment 3 of PFL. Among the φ-sets compatible with that hypothesis we chose those whose $\langle(\Delta\rho)^4\rangle$ is minimum (with the exception of experiment 4, where we adopted the second best, on the ground that the indices of local sphericity are slightly small; the difference bears on the weakest reflection

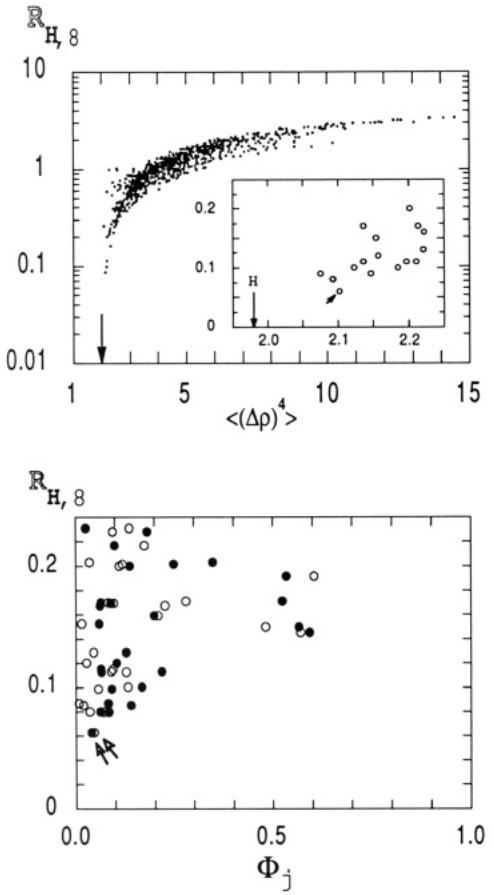

FIGURE 2: Search for the φ-set of phase Q^{227} whose histogram $\mathbb{H}(\Delta\rho)$ best fits the histogram of phase H. The apodized, extrapolated data of Table II were used. $\mathbb{R}_{H,8}$ and Φ_j are, respectively, the "distance" and the index of local sphericity as defined by eqs 2 and 3. The vertical arrow points at the value of $\langle(\Delta\rho)^4\rangle$ for phase H. PFL, experiment 3. Upper panel: plot of $\mathbb{R}_{H,8}$ vs $\langle(\Delta\rho)^4\rangle$ (every 10th point). Inset: same plot, expanded to display all the φ-sets whose $\langle(\Delta\rho)^4\rangle$ is close to phase H. Lower panel: plot of $\mathbb{R}_{H,8}$ vs Φ_j at the points a (solid symbols) and c (open symbols). The points corresponding to the "best" φ-set are marked by small arrows.

(620) whose sign has but a tiny influence on the map).

The maps corresponding to the six experiments are reported in Figure 3. The most striking feature is the presence, in all the maps, of two types of disjointed micelles, quasi-spherical in shape.

Discussion and Conclusions

From a formal crystallographic viewpoint, the structure can be described in terms of two types of disjointed globular elements (Figure 4). Eight (per F-centered cubic cell), of symmetry $\bar{4}3m$, are centered at positions a, and 16, of symmetry $\bar{3}m$, are centered at positions d (*International Tables*, 1952). As discussed by Mariani et al. (1990), the structure is of type II: the interior of the globules is filled by the polar moiety (water and polar headgroups of the lipid molecules), and the hydrocarbon chains form a continuous 3D matrix. The values of the indices Φ_a and Φ_d (Table II) indicate that the two types of globular elements display a high degree of spherical symmetry.[3] It can be noted in the maps (Figure 3) that the diameter of the globules a is larger than that of

[3] The indices Φ_b and Φ_c, relevant to the points b and c, which are crystallographically distinct from but have the same symmetry as the points a and d (*International Tables* 1952), take values close to 1 (results not shown).

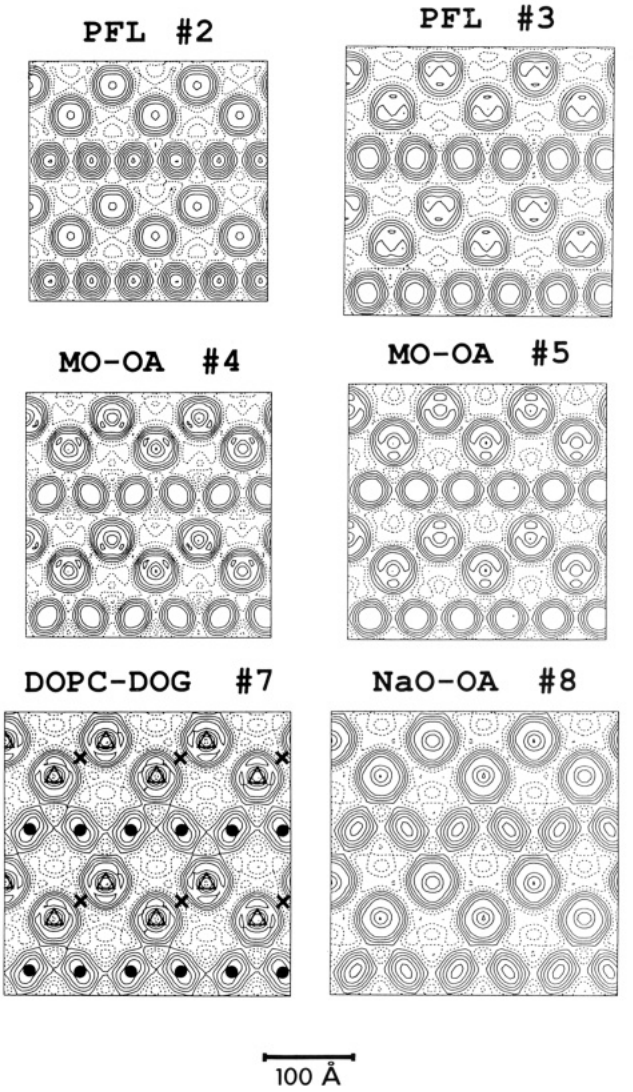

FIGURE 3: Electron density maps $\Delta\rho(x,y,z)$; (110) sections through the center of symmetry for six of the experiments of Table I. The maps correspond to the structure factors of Table II. The separation of the equidensity lines is 0.5; the negative levels are dotted. Note the presence of two types of disjointed micelles, centered respectively at the points a (open triangles) and d (solid dots). A cross marks the position of a center of symmetry.

the globules d and also that the electron density has a minimum at the center of globules a, whose depth increases with the amount of water. This and other points of chemical interest will be discussed more thoroughly elsewhere.

Q^{227} is the first 3D periodically ordered micellar organization of type II reported in lipid-containing systems. A micellar organization of type I has been proposed for another cubic phase [Q^{223}, Eriksson et al. (1987); a controversy regarding that phase is reviewed in Mariani et al. (1988)]. The four other cubic phases known so far are all bicontinuous; one (Q^{212}) contains, moreover, micelles of type II (Mariani et al., 1988). As a result of a formal geometric analysis of the assemblies of frustrated films, Charvolin and Sadoc (1988) have put forward, with remarkable insight, a description of the structure of phase Q^{227} in terms of a space-filling packing of quasi-regular 12- and 16-hedra. This description is consistent with the structure put forward in this work.

As in other recent publications from our laboratory (Luzzati et al., 1988; Mariani et al., 1988, 1990), the crystallographic procedure is based upon the axiom that the histogram of the electron density map is invariant with respect to physical structure but strongly dependent upon chemical composition.

Table II: Crystallographic Data Used in the Computation of the Maps[a]

lipid:	PFL	PFL	MO–OA	MO–OA	DOPG–DOG	NaO–OA
expt no.:	2	3	4	5	7	8
a (Å)	129.6	146.2	134.0	139.8	156.4	155.0
$F(111)$	+32	+30	−40	−25	−26	−47
$F(220)$	−127	−122	−112	−133	−108	−119
$F(311)$	−150	−146	−143	−124	−135	−141
$F(222)$	+140	+136	+135	+154	+101	+115
$F(400)$	+80	+85	+84	+99	+94	+88
$F(331)$	−32	−32	−35	−43	−49	−48
$F(422)$	−17	−17	−32	−35	−54	−39
$F(511)$	−18	−21	−29	−27	−42	−33
$F(333)$	−32	−36	−50	−47	−73	−57
$F(440)$	−30	−38	−52	−49	−76	−57
$F(531)$	0	+14	0	0		
$F(442)$	0	+14	0	−13		
$F(620)$	−16	−22	−21	+6		
$F(533)$		+17	0	+13		
$F(622)$		−19	−32	−27		
$2\beta^2$ (Å^2)	0	0	0	0	0	0
$-p\beta''(0)$ (10^{-3} Å^{-2})	9.12	7.98	10.10	9.13	8.10	7.27
γ/Γ	13/512	9/8192	4/1024	12/4096	1/256	3/256
$\langle(\Delta\rho)^4\rangle$	2.826	2.236	2.051	2.015	1.958	2.074
Φ_d	0.012	0.024	0.060	0.079	0.148	0.106
Φ_a	0.021	0.031	0.011	0.031	0.111	0.069
			Apodized Data			
$2\beta^2$ (Å^2)	−929	−490				
$-p\beta''(0)$ (10^{-3} Å^{-2})	10.5	8.88				
γ/Γ	9/512	6/8192				
$\langle(\Delta\rho)^4\rangle$	2.423	2.103				
Φ_d	0.035	0.040				
Φ_a	0.035	0.047				
$R_{H,8}$ (10^{-2})	15	6				

[a] The amplitudes of the structure factors correspond to the intensities reported in Table I, normalized to $\sum_{\mathbf{h}}|F(\mathbf{h})|^2 = 10^6$. The intensity of the Debye–Scherrer ring $h^2 + k^2 + l^2 = 27$ was shared between the reflections (511) and (333) as in Mariani et al. (1990). $p\beta''(0)$ is the curvature of the autocorrelation function at $r = 0$, Γ is the total number of φ-sets, γ is the rank of the φ-set in the list sorted according to increasing $\langle(\Delta\rho)^4\rangle$, and Φ_d and Φ_a are the indices of local sphericity (see eq 3). The signs of the reflections are those of the maps of Figure 3 (see text). For experiments 2 and 3 the values of the parameters $2\beta^2$, $\langle(\Delta\rho)^4\rangle$, Φ_d, Φ_a and $R_{H,8}$ corresponding to the apodized data are also reported.

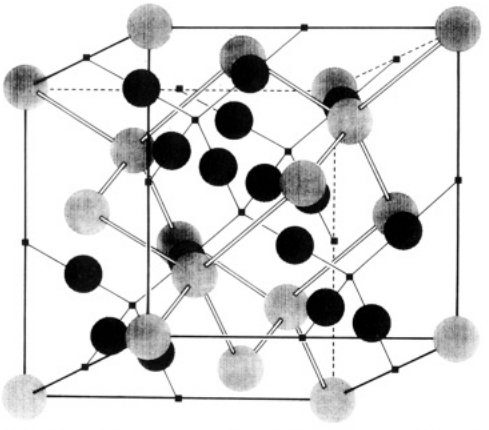

FIGURE 4: Schematic representation of the structure of the cubic phase. The space group is *Fd*3*m* [no. 227 (*International Tables*, 1952)]. The cube represents one face-centered cubic cell with origin choice 1 (note that the maps of Figure 3 are drawn with the origin choice 2). The structure consists of eight globules of symmetry $\bar{4}$3m (light grey), centered at positions a, and of 16 globules (dark grey) of symmetry $\bar{3}$m, centered at positions d. The full and the broken lines trace the two 3D lattices of phase Q^{224}, mutually intertwined and unconnected. Note that globules a are centered at the tetrahedral junctions of one of the networks of phase Q^{224}, and globules d are centered in the middle of the rods of the other network.

The implementation requires that two phases be observed, with the same chemical composition: one is the reference phase, whose structure is known, and the other is the unknown of the problem. In the case of phase Q^{227}, only PFL, of the numerous systems in which the phase was observed, fulfills that condition. *It is worthwhile to stress that, in the absence of a reference phase, hardly any crystallographic criterion would be available to sustain the structure analysis of the cubic phase.*

This paper rectifies a mistake: some lessons should be drawn from both the mistake and its correction. This is not the first time, in lipid literature, that errors are pointed out. Larsson (1983), for example, has discussed a case of a phase mixture wrongly interpreted as a single phase; another example of incorrect indexing is the cubic phase mentioned by Das and Rand (1986), which we now believe to be Q^{227}. We could draw other examples of incorrect indexing out of our own experience. In all those cases, nevertheless, and whenever the structure analysis was pursued using the incorrect data, the results could not be interpreted in terms of any chemically sensible structure. In the case of PFL, two unlikely circumstances concurred to make the error particularly difficult to spot. On the one hand, the cubic and the hexagonal phases are epitaxially related to each other; this is now known to be a highly significant event, related to the mechanisms of phase-transition processes (Rançon & Charvolin, 1987; Clerc et al., 1991). One the other hand, in the case of PFL the incorrect set of intensities yielded a map that prima facie seemed to make good chemical sense. In retrospect, we should have been more attentive to the anomalies reported by Mariani et al. (1990) hinting that some of the data might be at variance with the model.

This paper is sharply focused on the crystallographic aspects of the structure analysis. Other considerations of chemical, physical, and biological interest will be developed elsewhere.

Acknowledgments

We are grateful to T. Gulik-Krzywicki and to J. L. Nieva for the communication of unpublished observations.

Registry No. MO, 111-03-5; DOPC, 4235-95-4; DMPC, 18194-24-6; NaO, 143-19-1; OA, 112-80-1; MA, 544-63-8; DOG, 25637-84-7.

REFERENCES

Caffrey, M. (1989) *Annu. Rev. Biophys. Biophys. Chem. 18*, 159-186.
Charvolin, J., & Sadoc, J. F. (1988) *J. Phys. 49*, 521-526.
Clerc, M., Levelut, A. M., & Sadoc, J. F. (1991) *J. Phys.* (in press).
Das, S., & Rand, R. P. (1986) *Biochemistry 25*, 2882-2889.
Eriksson, P. O., Lindblom, G., & Arvidson, G. (1987) *J. Phys. Chem. 91*, 846-853.
Gulik, A., Luzzati, V., DeRosa, M., & Gambacorta, A. (1985) *J. Mol. Biol. 182*, 131-149.
Heimburg, T., Ryba, N. J. P., Würtz, U., & Marsh, D. (1990) *Biochim. Biophys. Acta 1025*, 77-81.
International Tables for X-ray Crystallography (1952) Kynoch Press, Birmingham, U.K.
Larsson, K. (1983) *Nature (London) 304*, 664.
Luzzati, V., Tardieu, A., & Taupin, D. (1972) *J. Mol. Biol. 64*, 269-286.
Luzzati, V., Mariani, P., & Delacroix, H. (1988) *Makromol. Chem., Macromol. Symp. 15*, 1-17.
Mariani, P., Luzzati, V., & Delacroix, H. (1988) *J. Mol. Biol. 204*, 165-189.
Mariani, P., Rivas, E., Luzzati, V., & Delacroix, H. (1990) *Biochemistry 29*, 6799-6810.
Rançon, Y., & Charvolin, J. (1987) *J. Phys. 48*, 1067-1073.
Seddon, J. M. (1990) *Biochemistry 29*, 7997-8002.
Seddon, J. M., Bartle, E. A., & Mingins, J. (1990a) *J. Phys. Condens. Matter 2*, SA285-SA290.
Seddon, J. M., Hogan, J. L., Warrender, N. A., & Pebay-Peyroula, E. (1990b) *Prog. Colloid Polym. Sci. 81*, 189-197.
Shyamsunder, E., Gruner, S. M., Tate, M. W., Turner, D. C., So, P. T. C., & Tilcock, C. P. S. (1988) *Biochemistry 27*, 2332-2336.
Tardieu, A. (1972) Thesis, Université Paris-Sud.

Structural Characterization of the *N*-Glycans of a Recombinant Hepatitis B Surface Antigen Derived from Yeast†

Charlotte C. Yu Ip,‡ William J. Miller,‡ and Dennis J. Kubek§

Department of Cellular and Molecular Biology and Biochemical Process Research and Development, Merck Sharp & Dohme Research Laboratories, West Point, Pennsylvania 19486

Anne-Marie Strang and Herman van Halbeek

Complex Carbohydrate Research Center and Department of Biochemistry, The University of Georgia, Athens, Georgia 30602

Susan J. Piesecki and Jack A. Alhadeff*

Department of Chemistry, Division of Biochemical Sciences, Lehigh University, Mountaintop Campus, Bethlehem, Pennsylvania 18015

Received June 12, 1991; Revised Manuscript Received August 29, 1991

ABSTRACT: The *N*-glycans of purified recombinant middle surface protein (preS2+S) from hepatitis B virus, a candidate vaccine antigen expressed in a mnn9 mutant strain of *Saccharomyces cerevisiae*, have been characterized structurally. The glycans were released by *N*-glycanase treatment, isolated by size-exclusion chromatography on Sephadex G-50 and Bio-Gel P-4 columns, and analyzed by 500-MHz ^{1}H NMR spectroscopy and fast atom bombardment mass spectrometry. The mixture of oligosaccharides was fractionated by HPLC, the major subfractions were isolated, and their carbohydrate compositions were determined by high-pH anion-exchange chromatography with pulsed amperometric detection. The combined results suggest that high-mannose oligosaccharides account for all the *N*-glycans released from preS2+S: structures include $Man_7GlcNAc_2$, $Man_8GlcNAc_2$, and $Man_9GlcNAc_2$ isomers in the ratios of 3:6:1. Approximately 80% of the oligosaccharides contain the C2,C6-branched trimannosyl structural element typical of yeast high-mannose oligosaccharides but not usually found in high-mannose oligosaccharides in animal glycoproteins.

Hepatitis B is a major disease chronically afflicting more than 300 million people worldwide (Blumberg & London, 1982; Stephenne, 1990). The disease is caused by a hepatotropic DNA virus designated hepatitis B virus (HBV)[1] (Chisari et al., 1989). Disease manifestations range from asymptomatic infection to chronic severe and progressive liver disease associated with high morbidity and mortality (Blumberg & London, 1982; Stephenne, 1990). Prolonged hepatitis B infection over many years can lead to cirrhosis and a significantly increased risk (200-fold) of developing hepatocellular carcinoma

† This investigation was supported in part by National Institutes of Health Grant P41-RR-05351 from the Division of Research Resources (to H.v.H.).

* Author to whom correspondence should be addressed.
‡ Department of Cellular and Molecular Biology, Merck Sharp & Dohme.
§ Biochemical Process Research and Development, Merck Sharp & Dohme.

[1] Abbreviations: DSS, sodium 4,4-dimethyl-4-silapentane-1-sulfonate; FABMS, fast atom bombardment mass spectrometry; HBsAg, hepatitis B surface antigen; HBV, hepatitis B virus; HPAEC, high-pH anion-exchange chromatography; HPLC, high-performance liquid chromatography; ORF, open reading frame; PAD, pulsed amperometric detection; PAGE, polyacrylamide gel electrophoresis; PEG, poly(ethylene glycol); SDS, sodium dodecyl sulfate; SEC, size-exclusion chromatography; TFA, trifluoroacetic acid; WEFT, water elimination Fourier transform.

0006-2960/92/0431-285$03.00/0